

Photoinduced electronic energy transfer in modular, conjugated, dinuclear Ru(II)/Os(II) complexes

Steve Welter^a, Nunzio Salluce^b, Peter Belser^b, Michiel Groeneveld^a, Luisa De Cola^{a,*}

^a *HIMS, Molecular Photonic Materials, Universiteit van Amsterdam, Nieuwe Achtergracht 166, 1018WV Amsterdam, The Netherlands*

^b *Department of Chemistry, University of Fribourg, Pérolles, Fribourg CH-1700, Switzerland*

Received 27 September 2004; accepted 19 November 2004

Available online 8 April 2005

Contents

1. Introduction	1361
2. Design and synthesis of the compounds	1361
3. Results and discussion	1363
3.1. Electronic absorption and emission properties	1363
3.2. Time-resolved spectroscopy	1364
3.3. Photoinduced energy transfer	1365
4. Conclusions	1367
5. Experimental	1368
5.1. Solvents and starting materials	1368
5.2. Instrumentation	1368
5.3. Spectroscopy	1368
5.4. Preparation of the complexes	1368
5.4.1. [Rubpy-ph ₃ -Si(CH ₃) ₃](PF ₆) ₂ (1)	1368
5.4.2. [Rubpy-ph ₃ -I](PF ₆) ₂ (2b)	1368
5.4.3. [Rubpy-ph ₄ -I](PF ₆) ₂ (2c)	1368
5.4.4. [Rubpy-ph ₃ -bpy](PF ₆) ₂ (3b)	1369
5.4.5. [Rubpy-ph ₄ -bpy](PF ₆) ₂ (3c)	1369
5.4.6. [Rubpy-ph ₅ -bpy](PF ₆) ₂ (3d)	1369
5.5. General procedure for the synthesis of heterodinuclear Ru/Os complexes	1369
5.5.1. [Ru-ph ₂ -Os](PF ₆) ₄ (4a)	1369
5.5.2. [Ru-ph ₃ -Os](PF ₆) ₄ (4b)	1369
5.5.3. [Ru-ph ₄ -Os](PF ₆) ₄ (4c)	1369
5.5.4. [Ru-ph ₅ -Os](PF ₆) ₄ (4d)	1369
5.6. Alternative synthetic route for	1370
5.6.1. [Ru-ph ₂ -Os](PF ₆) ₄ (4a)	1370
Acknowledgments	1370
References	1370

Abstract

Rigid, modular heterometallic dinuclear complexes containing luminescent units have been synthesized and their photophysical properties investigated. The metal complexes are derivatives of ruthenium and osmium trisbipyridine compounds and are linked by 2, 3, 4 or 5 *para*-phenylene units. A fast and efficient photoinduced energy transfer takes place from the excited ruthenium moiety to the osmium-based

* Corresponding author. Tel.: +31 20 525 6459; fax: +31 20 525 6456.

E-mail address: ldc@science.uva.nl (L. De Cola).

component. The rate constants of the energy transfer processes have been determined by time-resolved emission and sub-picosecond transient absorption spectroscopy. A comparison with similar systems containing substituted polyphenylene units is made in order to clarify the role of the tilt angle between the spacers on the energy transfer rates. Such investigation confirmed that a through bond Dexter type mechanism is responsible for the process.

© 2005 Elsevier B.V. All rights reserved.

Keywords: Dinuclear metal complex; Energy transfer; Ruthenium complexes; Osmium complexes; *para*-Phenylene; Luminescence

1. Introduction

Long-range energy and electron transfer processes are amongst the most interesting and challenging reactions both from a theoretical and an application perspective [1,2]. Different approaches related to the feasibility to construct long rigid systems where an electron or energy donor moiety is separated by a long connector to an acceptor system have been taken in the last few years [3,4]. In many cases to have a good control of the geometry, distance and stability, a covalent strategy, in synthesizing such dyads, has been successfully applied. Furthermore in order to cover a large distance of several nanometers, and to successfully compete with the excited state lifetime of the donor, luminescent, long lived metal complexes have been employed as energy and/or electron donor and acceptor components [5–10]. Such choice in fact allows, due to the “phosphorescent” character of the excited state, by an appropriate selection of the coordinated ligands, to achieve excited state lifetimes of the order of several hundred nanoseconds up to milliseconds. Furthermore the energy of the excited states and the redox properties of the ground and excited states can also be tuned allowing a thermodynamically control of the photoinduced processes. Ruthenium and osmium complexes have been largely employed as donor and acceptor units in covalently linked dyads [11–32] and the distance between the two components has been tuned using spacers of different length. In many cases however the electronic interaction through bond, between the terminal metal complexes, has been ascribed as the predominant mechanism for the transfer of charge or energy. Therefore for a fully understanding of the factors that influence the processes a modular approach is desirable and the use of conjugated versus saturated spacer could lead to long-range interactions.

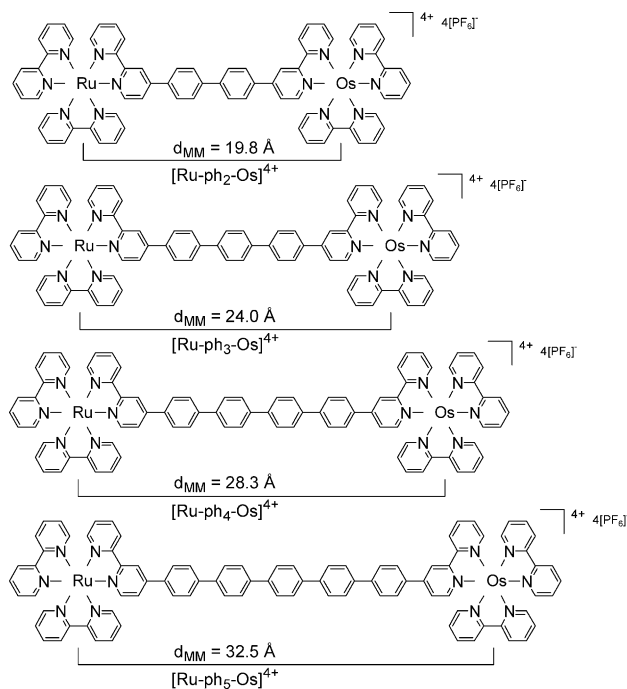
Amongst the available easily functionalizable aromatic species, oligophenylenes are surely the simplest and most widely available. However their use in the construction of dyads has been poorly investigated and it is restricted to only very few units (1–3 [25,33–37]), acting as spacers between the metal complexes components. In fact the problems related to their use lie in their low solubility in organic solvents, when they are not substituted. Only the small oligomers (1 or 2 phenylene units) are soluble enough to construct the bridging ligand that will allow the coordination of the metal units. On the other hand substitution with solubilizing groups lead to a decrease in their conjugation rendering them less appealing for the construction of systems for long-range energy or electron transport. We have overcome such a problem intro-

ducing a new strategy to construct modular long dinuclear heterometallic ruthenium and osmium complexes and in this paper we report the synthesis, characterization, and photophysical behaviour of such compounds. The metal centres $\text{Ru}(\text{bpy})_3^{2+}$ and $\text{Os}(\text{bpy})_3^{2+}$ (where $\text{bpy} = 2,2'$ -bipyridine) are separated by a bridging ligand that consists of 2, 3, 4, or 5 *para*-phenylene units. The modulation of the length will allow us to understand the way structural and energetic factors determine the rate and efficiency of the electronic energy transfer.

2. Design and synthesis of the compounds

All the compounds synthesized and investigated and their abbreviations are reported in Scheme 1.

As mentioned in Section 1 one of the aims of our work is to realize systems in which long-range energy or electron processes can take place. The rates and efficiencies of such processes depend on several structural and energetic factors that involve the donor unit, the acceptor moiety and of course the connecting ligand. The result of the combination of these

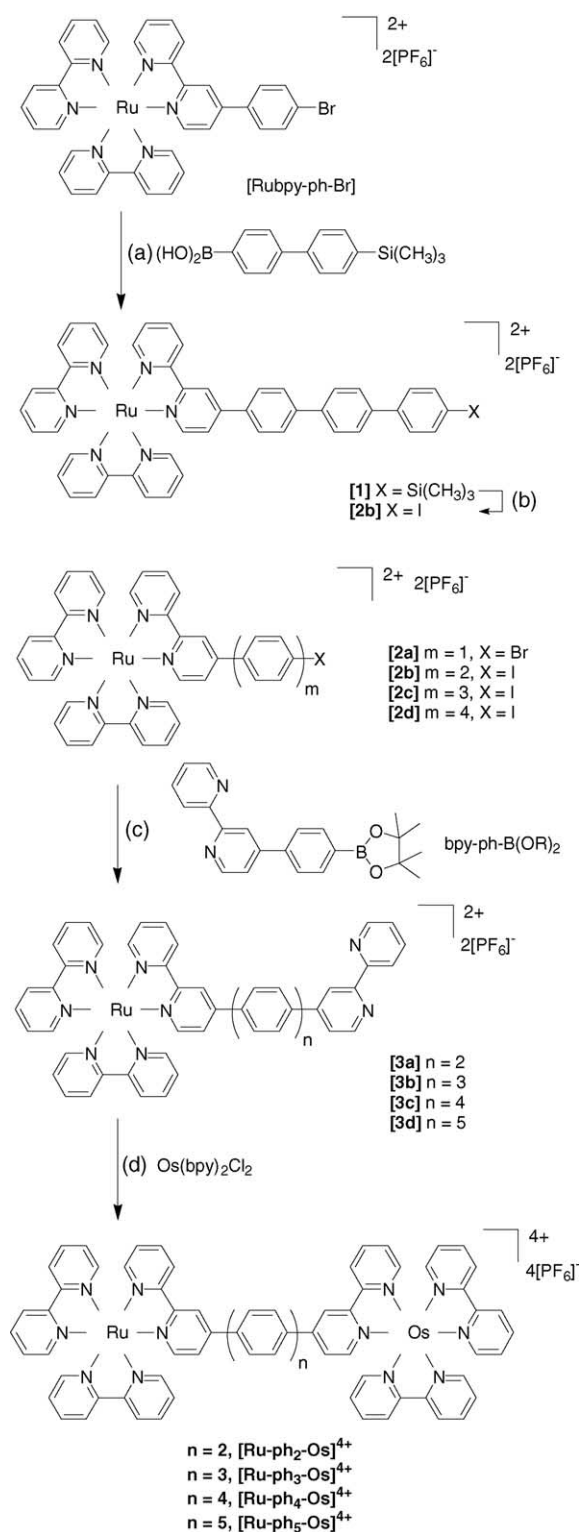


Scheme 1. Studied molecules and their abbreviations. The distance between the two metal centres is also shown.

factors is a good electronic interaction between the two metal centres and the realization of the desired wire-type behaviour [5,38]. The first requirement to be fulfilled in order to have an efficient energy transfer is the thermodynamic one; the process must be exoergonic ($\Delta G < 0$). Once such prerequisite is satisfied the rate will be determined by the distance between the chromophores, and if the mechanism of the process is through bond, by the electronic nature and geometry of the bridging ligand that will define the electronic coupling between the chromophores. The energy donor and acceptor components that we have chosen are $\text{Ru}(\text{bpy})_3^{2+}$ and $\text{Os}(\text{bpy})_3^{2+}$, respectively. Their photophysical properties are very well known [39] and they have been employed in many other dinuclear complexes [3,18,19,27,40–53].

One possible choice for the bridging ligand is to have an aromatic system of modular nature, so that the length can be easily changed. Furthermore the energy levels of the bridge should be higher than the acceptor energy levels in order to avoid having a trap for the energy localized on the bridge. Another important factor is the rigidity of the connecting unit. For the understanding of the mechanism of electronic energy transfer processes it is essential that the distance between the two reaction centres can be determined. For these reasons we decided to use *para*-phenylene units as spacers for the bridging ligand and 2,2'-bipyridine (bpy) as chelating units to coordinate the metal complexes acting as donor and acceptor moieties. We have already reported the synthesis of modular dinuclear Ru/Os systems connected by 3, 5 and 7 phenylene units [12]. However, in those systems, for synthetic reasons, the central phenylene was substituted with hexyl chains. Such substitution induced a tilt angle between the adjacent phenylenes of 60–65°. The rotation around the sigma bond perturbs the aromatic connectivity by reducing the conjugation of the bridging ligand and therefore decreasing the electronic coupling between the terminal metal complexes. We have therefore focused on a new synthetic route to eliminate the bulky solubilizing groups to reduce the tilt angle between the spacers and to demonstrate that indeed the planarization of the bridging ligand leads to a better intercomponent interaction, and faster intramolecular energy transfer.

For many long, modular systems the solubility of the ligand can represent a major problem for the synthesis of heterometallic complexes. Therefore the possibility to construct the bridging ligand from one of the metal centres can become an alternative appealing strategy to overcome the solubility problems. Such an approach has been successfully used for different systems [54,55]. We have decided to apply the same procedure for our dinuclear complexes containing polyphenylenes units. It is well known that polyphenylenes are insoluble in common organic solvents. However, using the “complex as ligands” strategy we were able, in a step-wise approach, to add by discrete units, as many spacers as desired. The charged metal unit is used in this case as solubilizing group. The coupling of a free chelating site to the bridge opens the possibility to complex a second metal centre. The synthetic procedure is sketched in Scheme 2 and all

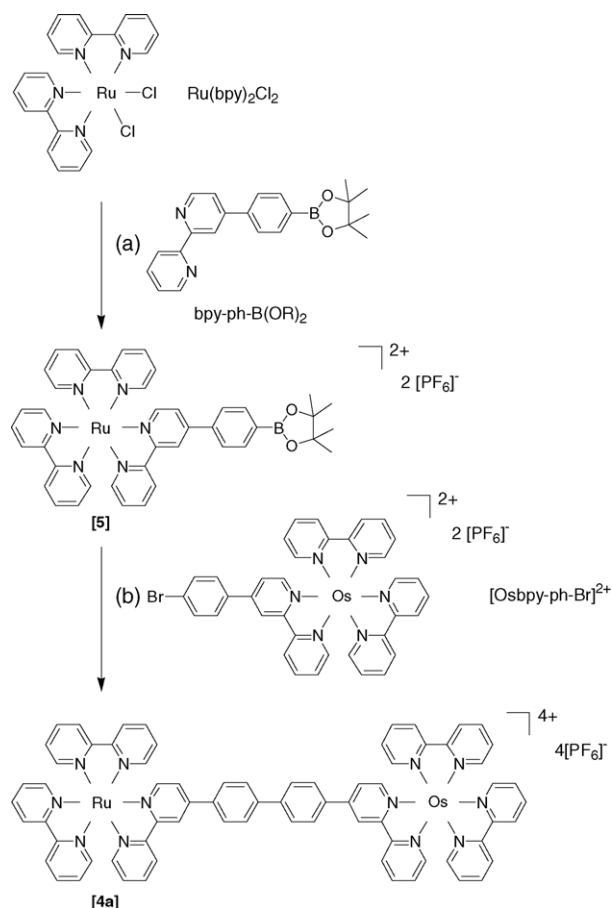


Scheme 2. Synthesis of the heterometallic $[\text{Ru-ph}_n\text{-Os}]^{4+}$ ($n = 2-5$) complexes using the $[\text{Ru}(\text{bpy})_n\text{-bpy}]^{2+}$ precursors: (a) K_2CO_3 , $\text{Pd}(\text{PPh}_3)_4$, DMF, 95 °C, 16 h, (b) ICl , CH_2Cl_2 , 0 °C, 1.5 h, (c) K_2CO_3 , $\text{Pd}(\text{PPh}_3)_4$, DMF, 95 °C, 6 h, (d) ethylene glycol, microwave irradiation (3×2 min, 450 W).

the details and characterization of the complexes are reported in Section 5.

The stepwise synthesis of ruthenium complexes containing a conjugated bridging ligand with a free bipyridine end is based on a successive two-step sequence. The first step implies the Suzuki coupling reaction between an aryl halide containing complex and a protected phenyl boronic acid. The second step consists of the cleavage of the trimethylsilyl group and iodation reaction with ICl at low temperature. Repetition of this two-step sequence leads to a modular construction of the phenylene spacer that is terminated by the coupling to a free bipyridine. The heterodinuclear complexes have been synthesized by the reaction between the $\text{Os}(\text{bpy})_2\text{Cl}_2$ precursor and the free bipyridine ligand of these complexes in ethylene glycol under microwave irradiation.

A second strategy is based on a direct coupling of two different metal centres by a cross-coupling reaction (see Scheme 3). We used the well-developed Pd(0) catalysed Suzuki cross-coupling reaction, involving an aryl halide and a boronic ester, to connect directly a ruthenium and an osmium centre. The complementarity between the two moieties allows the synthesis of heterometallic complexes in one step.



Scheme 3. Alternative synthetic way for the synthesis of $[\text{Ru-ph}_2\text{-Os}]^{4+}$ by direct coupling of a Ru-based unit and the complementary Os component: (a) methoxy ethanol, 90°C , 18 h; (b) DMF, K_2CO_3 , $\text{Pd}(\text{PPh}_3)_4$, 100°C , 22 h, 42%.

3. Results and discussion

3.1. Electronic absorption and emission properties

The UV–vis absorption spectra of the $[\text{Ru-ph}_n\text{-Os}]^{4+}$ complexes are shown in Fig. 1a. All the spectra were recorded at room temperature in air-saturated acetonitrile solutions. In the UV region the strong band at 290 nm is assigned to singlet intraligand (^1IL) $\pi\text{--}\pi^*$ transitions of the bipyridines. The band between 320 and 360 nm is due to a spin allowed $\pi\text{--}\pi^*$ transition localized on the phenylene bridge. With increasing number of phenyls the intensity of this band increases and the maximum shifts to lower energy accordingly with the well-known decrease of the HOMO–LUMO gap for conjugated units until the effective conjugation length is reached [56]. In the visible region around 440 nm the characteristic singlet metal-to-ligand charge transfer ($^1\text{MLCT}$) bands for $\text{Ru}(\text{bpy})_3^{2+}$ and at slightly lower energy those for $\text{Os}(\text{bpy})_3^{2+}$ derivatives are observed. A weaker absorption between 560 and 680 nm can be assigned to the spin forbidden $^3\text{MLCT}$ transition involving the osmium units and are due to the strong spin–orbit coupling promoted by the heavy metal. A comparison between the absorption spectra of one of the heterometallic complexes, $[\text{Ru-ph}_4\text{-Os}]^{4+}$ and the absorption spectra of $[\text{Ru-ph}_4\text{-Ru}]^{4+}$ and $[\text{Os-ph}_4\text{-Os}]^{4+}$ is shown

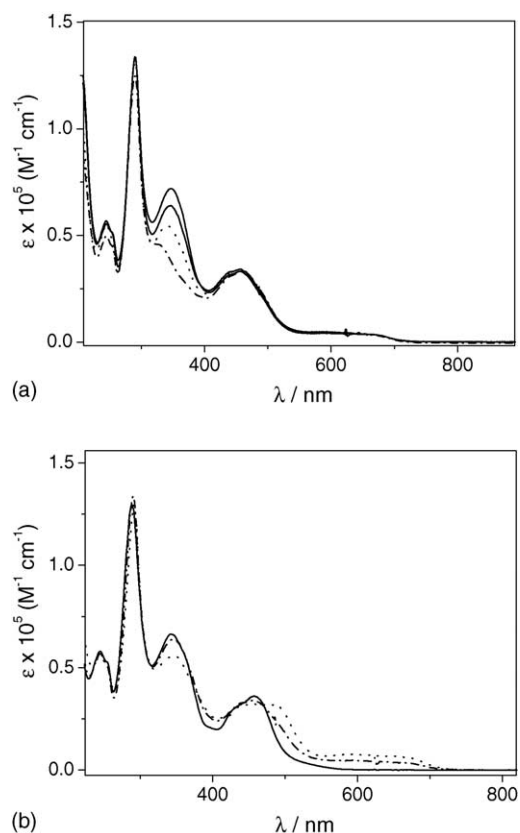


Fig. 1. Absorption spectra of (a) $[\text{Ru-ph}_2\text{-Os}]^{4+}$ (---), $[\text{Ru-ph}_3\text{-Os}]^{4+}$ (···), $[\text{Ru-ph}_4\text{-Os}]^{4+}$ (- · -) and $[\text{Ru-ph}_5\text{-Os}]^{4+}$ (—), (b) $[\text{Ru-ph}_4\text{-Ru}]^{4+}$ (—), $[\text{Os-ph}_4\text{-Os}]^{4+}$ (···), and $[\text{Ru-ph}_4\text{-Os}]^{4+}$ (- · -) in acetonitrile at room temperature.

Table 1
 Luminescence data

	298 K ^a				77 K ^b			
	Ru		Os		Ru		Os	
	λ_{\max} (nm)	τ (ps)	λ_{\max} (nm)	τ (ns)	λ_{\max} (nm)	τ (ns)	λ_{\max} (nm)	τ (μ s)
[Ru-ph ₂ -Os] ⁴⁺	^c	4 ^d	752	43	592	^{e,f}	715	1.1
[Ru-ph ₃ -Os] ⁴⁺	620	17 ^d	751	43	591	0.1 ^f	715	1.2
[Ru-ph ₄ -Os] ⁴⁺	617	245 ^d	753	43	591	0.4 ^f	715	1.1
[Ru-ph ₅ -Os] ⁴⁺	621	2020	751	43	594	0.7 ^f	715	1.1
[Ru-ph ₄ -Ru] ⁴⁺	625	206 \times 10 ³	—	—	595	6.4 \times 10 ³	—	—
[Os-ph ₄ -Os] ⁴⁺	—	—	746	39	—	—	719	1.0

^a In air equilibrated acetonitrile, $\lambda_{\text{exc}} = 450$ nm.

^b In butyronitrile glass, $\lambda_{\text{exc}} = 450$ nm.

^c Too low in intensity to be determined accurately.

^d $\lambda_{\text{exc}} = 420$ nm.

^e Too fast to be detected by our experimental setup.

^f $\lambda_{\text{exc}} = 324$ nm.

in Fig. 1b. It can be seen that the absorption spectrum of the heterodinuclear [Ru-ph₄-Os]⁴⁺ is equal to a spectrum of a 1:1 mixture of the parent homodinuclear complexes [Ru-ph₄-Ru]⁴⁺ and [Os-ph₄-Os]⁴⁺. This is an indication that a weak electronic interaction between the metal centres is present. The three spectra show an isosbestic point at about 440 nm in which the Ru and Os components absorb the same fraction of incident light. Such an observation will be useful for the quantitative evaluation of the quenching and sensitisation processes due to electronic energy transfer in the heterodinuclear complexes (see Section 3.3).

The emission properties of all the complexes were investigated at 293 K in acetonitrile solutions and at 77 K in butyronitrile rigid matrix upon excitation at 440 nm. The photophysical data are summarized in Table 1. The room-temperature emission spectra of the [Ru-ph_{*n*}-Os]⁴⁺ derivatives (*n* = 2–5) and, for comparison, of [Ru-ph₄-Ru]⁴⁺ are shown in Fig. 2. The spectra of [Ru-ph_{*n*}-Os]⁴⁺ and of [Ru-ph₄-Ru]⁴⁺ have been obtained with diluted solutions (optical density < 0.1) and the same absorption at the excitation wavelength. It can be seen that the emission of the ruthenium com-

ponent for [Ru-ph₄-Os]⁴⁺ is almost completely quenched due to intercomponent energy transfer. A full sensitisation of the osmium emission is observed and the osmium unit emits at 750 nm with its own unchanged quantum yield. At 77 K in butyronitrile rigid matrix the emission maxima are blue-shifted compared to the emission at 293 K. This is consistent with the charge-transfer nature of the emitting exciting state and the lack of solvent stabilization in rigid matrix. Also at 77 K the occurrence of intramolecular electronic energy-transfer processes can be observed even though in such a case a quantitative estimation of the emission quantum yields was not possible. The process has an efficiency of almost 100% and the rates of the process have been estimated by time-resolved spectroscopy (see next section).

3.2. Time-resolved spectroscopy

A more precise evaluation of the degree of quenching and the calculation of the rate of the photoinduced process was carried out with time-resolved emission, and in the cases in which the ruthenium-based component emission was too weak by sub-picosecond transient absorption spectroscopy. The osmium-based emission excited state lifetimes were determined using a Coherent Infinity Nd:YAG-XPO laser and a Hamamatsu C5680-21 streak camera ($\lambda_{\text{ex}} = 450$ nm). All the measurements were performed in air-equilibrated acetonitrile. The results are reported in Table 1. The lifetimes of the osmium-based emission for all the [Ru-ph_{*n*}-Os]⁴⁺ compounds are similar to the lifetime obtained for the reference complex [Os-ph₄-Os]⁴⁺ [57] and for [Os(bpy)₃]²⁺ [58]. In the case of the ruthenium-based emission the lifetimes are strongly reduced in comparison to the parent complex [Ru-ph₄-Ru]⁴⁺ [57].

For the complex with the shortest spacer ([Ru-ph₂-Os]⁴⁺) the lifetime of the ruthenium-based component is decreased to 4 ps as compared to [Ru-ph₄-Ru]⁴⁺ that exhibits a lifetime of 206 ns. By increasing the length of the *para*-phenylene spacer the excited state lifetimes of the ruthenium also in-

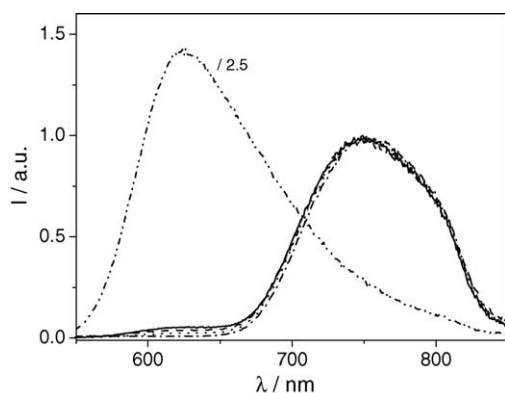


Fig. 2. Luminescence spectra of [Ru-ph₂-Os]⁴⁺ (---), [Ru-ph₃-Os]⁴⁺ (···), [Ru-ph₄-Os]⁴⁺ (- · -), [Ru-ph₅-Os]⁴⁺ (—) and [Ru-ph₄-Ru]⁴⁺ (— · —) in acetonitrile at room temperature ($\lambda_{\text{ex}} = 440$ nm).

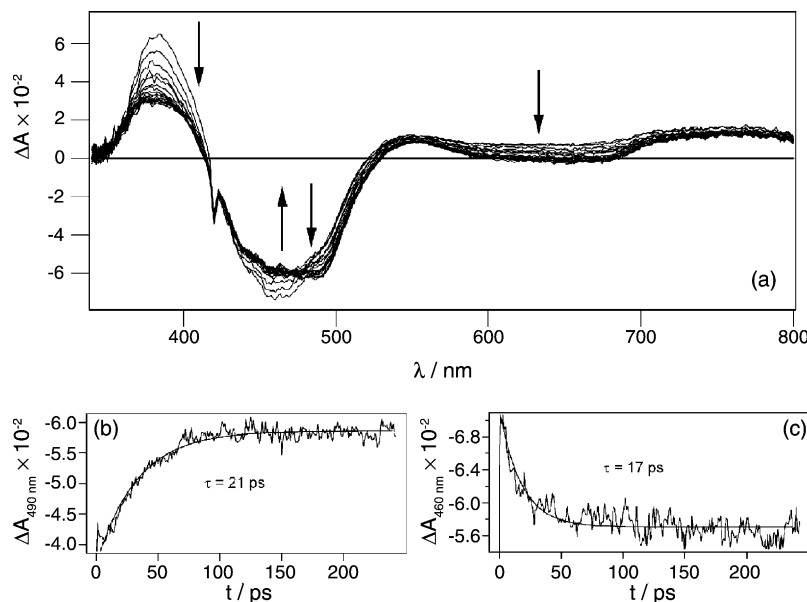


Fig. 3. Sub-picosecond transient absorption spectrum (a) of $[\text{Ru-ph}_3\text{-Os}]^{4+}$ in acetonitrile ($\lambda_{\text{ex}} = 420 \text{ nm}$), (b) rise-time at 490 nm, (c) decay time at 460 nm.

crease up to a value of 2 ns for the longest complex $[\text{Ru-ph}_5\text{-Os}]^{4+}$. In Fig. 3 the transient absorption spectrum of $[\text{Ru-ph}_3\text{-Os}]^{4+}$ is shown. The excitation wavelength of 420 nm was chosen to excite as much as possible into the $^1\text{MLCT}$ of the ruthenium. Although, it is impossible to avoid a simultaneous direct population of the excited state of the osmium since the absorption spectrum of the osmium component strongly overlaps with the ruthenium-based component. The transient absorption spectra show a band at 380 nm that is attributed to the radical anion $\text{bpy}^{\bullet-}$, a ground-state bleach in the region 410–520 nm and the large transient absorption band between 540 and 800 nm [57] is hidden by a bleaching. The positive band, if visible, is assigned to the delocalization of the radical anion $\text{bpy}^{\bullet-}$ over the *para*-phenylene spacer. Indeed the lowest excited state derives from a metal to ligand charge transfer to the bipyridine with the lowest reduction potential, in this case the bpy substituted with the conjugated *para*-phenylene spacer. In the region between 580 and 690 nm however also the ground-state bleaching band arising from the spin-forbidden $^3\text{MLCT}$ of the osmium can be seen. Over time the maximum of the ground-state bleaching band around 460 nm is shifting to the red by 30 nm. We attribute this shift to a direct observation of electronic energy transfer from the excited state of the ruthenium to the MLCT of the osmium. The decay of the band at 460 nm of 17 ps (Fig. 3c) corresponds to the formation of the band, rise time, at 490 nm (21 ps, Fig. 3b). The same rise time is obtained monitoring the formation of the bleaching at about 650 nm characteristic of the Os(II) unit.

3.3. Photoinduced energy transfer

The energy transfer process can be schematically represented by the energy-level diagram for the heterodinuclear $[\text{Ru-ph}_n\text{-Os}]^{4+}$ derivatives ($n=2\text{--}5$) and is depicted

in Fig. 4. The energies of the lowest spin-allowed MLCT for the metal-based components were obtained from the maximum of the corresponding absorption bands, whereas the energy for the lowest spin-forbidden MLCT excited state was obtained from the maximum of the emission band at 77 K. The energy transfer process is exoergic with $\Delta G = -0.37 \text{ eV}$ as calculated from the triplet state energies of the ruthenium ($^3\text{MLCT}_{\text{Ru}} = 2.10 \text{ eV}$) and osmium component ($^3\text{MLCT}_{\text{Os}} = 1.73 \text{ eV}$), respectively.

The energy of the triplet excited state of the *para*-phenylene spacer is not known exactly but we believe that it is higher in energy than the lowest excited states of both ruthenium and osmium. The energy of the triplet excited state is $22,900 \text{ cm}^{-1}$ for biphenyl and $20,400 \text{ cm}^{-1}$ for *para*-terphenyl [59,60]. If the energy of the lowest excited triplet

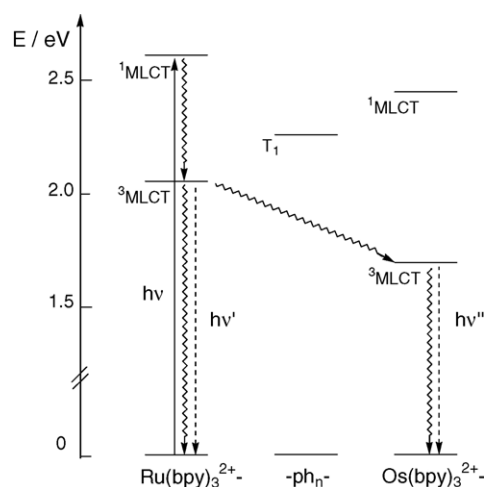


Fig. 4. Schematic energy-level diagram for the $[\text{Ru-ph}_n\text{-Os}]^{4+}$ ($n=2\text{--}5$) complexes.

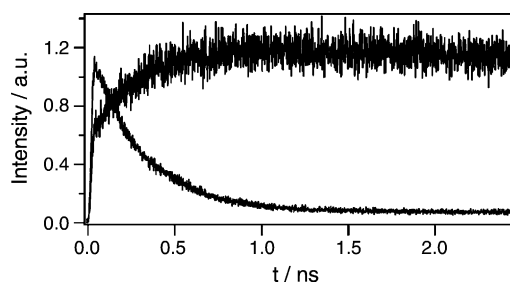


Fig. 5. Time-resolved emission of $[\text{Ru-ph}_4\text{-Os}]^{4+}$ in aerated acetonitrile ($\lambda_{\text{exc}} = 324 \text{ nm}$), showing the decay at 620 nm, ruthenium moiety (245 ps), and the rise time at 740 nm, osmium moiety (251 ps).

decreases as $1/n$, as it is known to happen for the maximum of the lowest energy absorption band, and the singlet–triplet separation remains constant, it can be estimated that the energy of the lowest excited triplet is around $19,600 \text{ cm}^{-1}$ for tetraphenyl and $19,000 \text{ cm}^{-1}$ for pentaphenyl. An indication that the triplet excited state is at higher energy is demonstrated by the fact that no quenching of the excited state lifetimes is observed in the parent homodimetallic complexes $[\text{Ru-ph}_n\text{-Ru}]^{4+}$ [57]. The conditions under which the experiments were carried out, low concentration ($\sim 3 \times 10^{-5} \text{ M}$) and rather short lifetimes ($< 250 \text{ ns}$), allow us to exclude intermolecular energy transfer processes. For the longer heterometallic compound, $[\text{Ru-ph}_4\text{-Os}]^{4+}$ and $[\text{Ru-ph}_5\text{-Os}]^{4+}$ the energy transfer process can be monitored by time-resolved emission spectroscopy. As can be seen in Fig. 5 the decay time monitored at 620 nm, on the ruthenium moiety, and the rise time, monitored at 740 nm have the same value and are a clear confirmation that the quenching of the ruthenium emission is due to a very efficient energy transfer process.

The rate constants for the energy transfer process can be calculated from the equation

$$k_{\text{en}} = \left(\frac{1}{\tau} \right) - \left(\frac{1}{\tau^0} \right) \quad (1)$$

where τ and τ^0 are the lifetimes of the quenched and unquenched ruthenium based luminescence, respectively. The rate constants are reported in Table 2. In order to establish the role of the bridging ligand and to determine the mechanism of the process a comparison with very similar complexes ($[\text{Ru-ph}_n\text{-Os}]^{4+}$) [12] in which the central phenylene unit is substituted by a hexyl chain (see Scheme 4) is discussed. In both series of complexes the driving force ($\Delta G = -0.37 \text{ eV}$) and

Table 2
Energy transfer rates^a

	$[\text{Ru-ph}_n\text{-Os}]^{4+}$		$[\text{Ru-ph}_n\text{R-Os}]^{4+}$	
	$k_{\text{en}} \text{ (s}^{-1}\text{)}$	$\ln(k_{\text{en}})$	$k_{\text{en}} \text{ (s}^{-1}\text{)}$	$\ln(k_{\text{en}})$
$[\text{Ru-ph}_2\text{-Os}]^{4+}$	2.5×10^{11}	26.2	—	—
$[\text{Ru-ph}_3\text{-Os}]^{4+}$	5.9×10^{10}	24.8	6.7×10^8	20.3
$[\text{Ru-ph}_4\text{-Os}]^{4+}$	4.1×10^9	22.1	—	—
$[\text{Ru-ph}_5\text{-Os}]^{4+}$	4.9×10^8	20.0	1.0×10^7	16.1
$[\text{Ru-ph}_7\text{-Os}]^{4+}$	—	—	1.3×10^6	14.1

^a In aerated acetonitrile solution.

the distance for the heterometallic compounds containing 3 or 5 phenylene spacers is the same. The only important difference is the tilt angle between the phenylene units, about 65° in the $[\text{Ru-ph}_n\text{R-Os}]^{4+}$ and 20° in the $[\text{Ru-ph}_n\text{-Os}]^{4+}$ family. The presence of the bulky alkyl chains induces an increase of the tilt angle between the phenyl rings and therefore reduces the electronic communication along the phenylene spacers, between the donor and acceptor moieties. Such small geometrical differences influence dramatically the rate of the energy transfer process since for $n = 3$ a 90-fold increase for the energy transfer process is obtained by planarization of the bridging ligand (see Table 2 and Scheme 4). It is interesting to notice that for the longer spacer with 5 phenylene units the difference for the energy transfer rate becomes smaller. In this case only a 50 times faster rate constant is observed for $[\text{Ru-ph}_5\text{-Os}]^{4+}$ compared to $[\text{Ru-ph}_5\text{R-Os}]^{4+}$. A possible explanation for the different ratio of the rates is that in the case of the $[\text{Ru-ph}_n\text{-Os}]^{4+}$ only the central phenylene is substituted with the bulky hexyl chain causing in that part of the chain a decrease of conjugation and therefore a “barrier” for the energy transfer process. In the shortest bridging ligand (smaller number of phenyls) the effect is apparently larger because the entire system is out of planarity.

Such a result clearly indicates that the energy transfer proceeds via a Dexter mechanism [61]. The different electronic coupling, due to the increase in planarity of the phenylenes in our systems, is the cause of a very fast and efficient energy transfer since the distance between the chromophores is the same for both series of complexes.

Since as already mentioned the excited states of the bridging ligand are too high in energy to be directly involved in the energy transfer process the attenuation factor β can be estimated by plotting the logarithm of the rates versus the distance between the donor and acceptor units. For comparison also the data obtained for the $[\text{Ru-ph}_n\text{R-Os}]^{4+}$ complexes [12] are reported in Fig. 6. The attenuation factors obtained for both systems are almost similar within experimental error but the rates for the unsubstituted phenylene

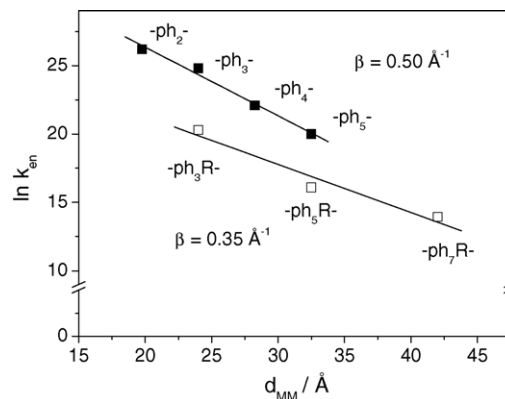
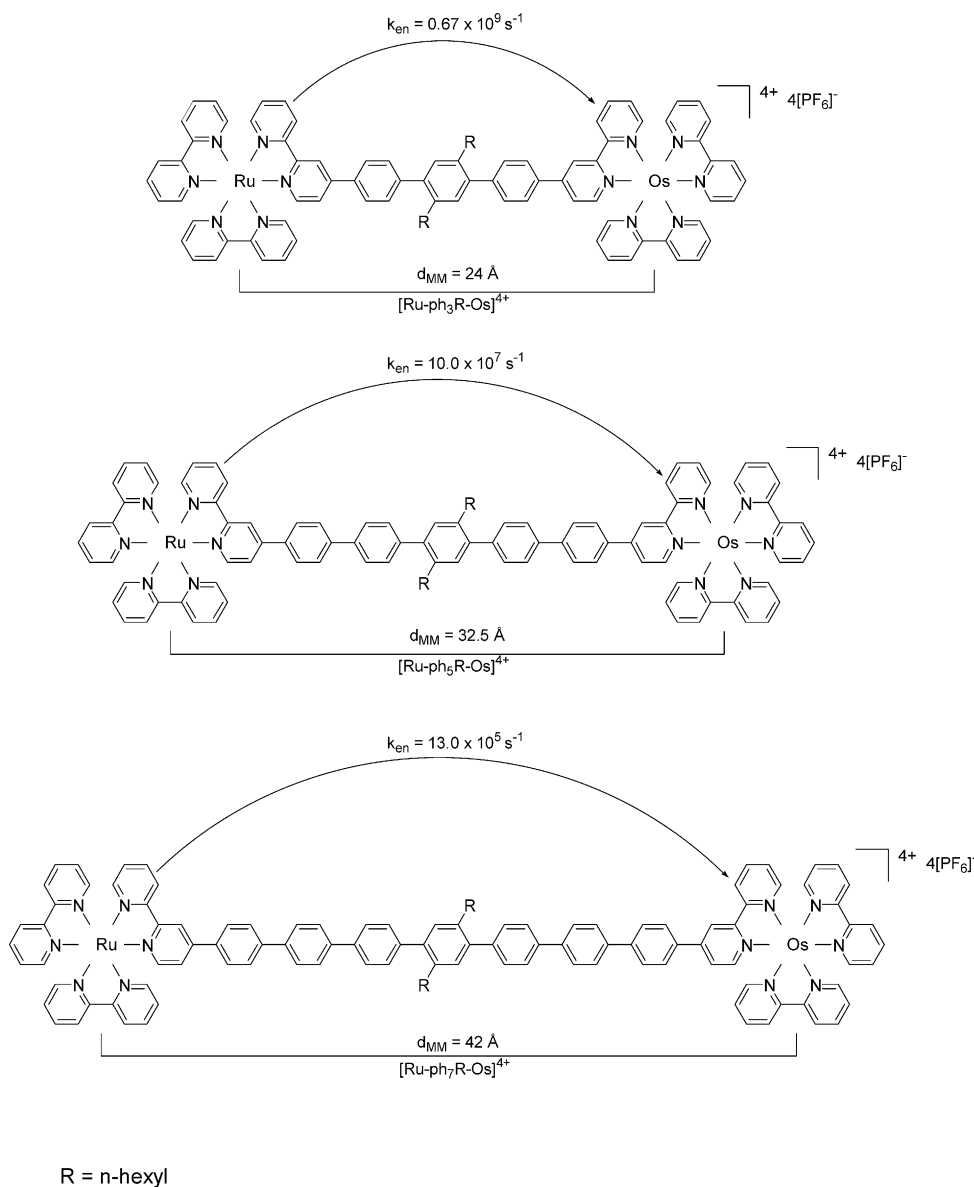


Fig. 6. Plot of $\ln(k_{\text{en}})$ vs. the metal–metal distance: (■) $[\text{Ru-ph}_n\text{-Os}]^{4+}$ complexes with bare phenylene bridge, (□) $[\text{Ru-ph}_n\text{R-Os}]^{4+}$ complexes with n -hexyl chains on the phenylene bridge.



Scheme 4. Schematic representation of the $[\text{Ru-ph}_n\text{R-Os}]^{4+}$ ($n = 3, 5, 7$; $\text{R} = n\text{-hexyl}$) complexes with the metal–metal distances (d_{MM}) and the energy transfer rate constants (k_{en}) [12].

bridges are higher. As can be seen the β value of 0.50 \AA^{-1} is in a very good agreement with similar systems containing polyphenylenes substituted in *para* position. Barigelletti et al. reported an attenuation factor of 0.33 \AA^{-1} for a cyclometalated $\text{Ru(II)}/\text{Os(II)}$, $(\text{ttp})\text{Ru}(\text{dpb}-(\text{ph})_n\text{-dpb})\text{Os}(\text{ttp})$ ($n = 0\text{--}2$), where the biscyclometalating bridging ligands contain dipyritylbenzene (dpb) fragments [25]. Interestingly similar attenuation factor values were obtained for electron transfer (ET) processes. McLendon and coworkers [62] found $\beta_{\text{ET}} = 0.4 \text{ \AA}^{-1}$, whereas Wasielewski and coworkers [63] reported $\beta_{\text{ET}} = 0.46 \text{ \AA}^{-1}$ for photoinduced electron transfer through phenylene spacers. Similar values ($\beta_{\text{ET}} = 0.61 \text{ \AA}^{-1}$) were also reported for the conductance of thin-films made of oligophenylene thiols [64]. This coincidence of β values for the energy and electron transfer may be fortuitous since

the energy transfer takes place according to a Dexter mechanism which formally consists of a double electron exchange. Therefore the distance dependence of the two electronic coupling matrix elements is expected to be different for energy and electron transfer processes.

4. Conclusions

We have synthesized and investigated a series of dinuclear heterometallic complexes containing *para*-polyphenylene units as spacers. The photophysical behaviour of such compounds clearly shows that an efficient and fast energy transfer takes place from the excited ruthenium-based component to the energy acceptor, osmium unit. A comparison with

analogous complexes containing substituted (twisted) phenylene units suggests that the geometry of the bridging ligand is important for the rates of the process. Furthermore the energy transfer process follows a Dexter-type mechanism.

5. Experimental

5.1. Solvents and starting materials

All reagents were purchased from Aldrich or Acros and used without purification unless otherwise indicated. Commercial deuterated solvents were used as received for the characterization of the compounds. Butyronitrile used for spectroscopy or electrochemistry was freshly distilled from CaH_2 before use. The procedure for the preparation of 4[4(4,4,5,5-tetramethyl-[1,3,2]dioxaborolan-2-yl)-[2,2']bipyridinyl (bpy-ph-B(OR)₂), [Os(bpy-ph₂-Br)(PF₆)₂], [Rubpy-ph₂-bpy](PF₆)₂, [57] Os(bpy)₂Cl₂, [65] 4'-trimethylsilylbiphenyl-4-boronic acid [66] and the synthesis of the Ru complexes [Rubpy-ph-Br](PF₆)₂, [Rubpy-ph₂-I](PF₆)₂ and [Rubpy-ph₄-Si(CH₃)₃](PF₆)₂ [67] are described elsewhere. All the complexes have been isolated as PF₆[−] salts. The complexes have been purified by column chromatography and characterized by ¹H NMR and mass spectroscopy.

5.2. Instrumentation

Proton NMR spectroscopy was performed at 300 MHz on a Varian Mercury 300 spectrometer, using solvents as internal references. Chemical shifts (δ) are reported in ppm downfield from tetramethylsilane and the residual nondeuterated solvent was used as reference. Electron spray ionization (ESI) mass spectra were measured with a Bruker FTMS 4.7 T Bio APEXII spectrometer.

5.3. Spectroscopy

The UV–vis absorption spectra were recorded on a Hewlett-Packard diode array 8453 spectrophotometer. Recording of the emission spectra was done with a SPEX 1681 Fluorolog spectrofluorometer. Low temperature emission spectra for glasses and solid state samples were recorded in 5 mm diameter quartz tubes that were placed in a Dewar filled with liquid nitrogen and equipped with quartz walls. The emission spectra were corrected for monochromator and photomultiplier efficiency. Lifetimes were determined using a Coherent Infinity Nd:YAG-XPO laser (1 ns pulses FWHM) and a Hamamatsu C5680-21 streak camera equipped with a Hamamatsu M5677 low speed single sweep unit.

A sub-nanosecond single photon counting setup was used for time-resolved fluorescence measurements. The excitation source consists of a frequency doubled (300–340 nm, 1 ps, 3.8 MHz) output of a cavity dumped DCM dye laser (Coherent model 700) that was pumped by a mode-locked Ar-ion laser (Coherent 486 AS Mode Locker, Coherent Innova 200

laser). A micro-channel plate photomultiplier (Hamamatsu R3809) was used as detector.

Sub-pico transient absorption spectroscopy experiments were based on a Spectra-Physics Hurricane titanium:sapphire regenerative amplifier system. The optical bench assembly of the Hurricane includes a seeding laser (Mai Tai), a pulse stretcher, a titanium:sapphire regenerative amplifier, a Q-switched pump laser (Evolution) and a pulse compressor. The 800 nm output of the laser is typically 1 mJ/pulse (130 fs) at a repetition rate of 1 kHz. A full-spectrum setup based on an optical parametric amplifier (Spectra-Physics OPA 800) as pump and residual fundamental light (150 μJ /pulse) from the pump OPA was used for white light generation, which was detected with a CCD spectrometer. The white light generation was accomplished by focusing the fundamental (800 nm) into a H₂O flow-through cell (10 mm).

5.4. Preparation of the complexes

5.4.1. [Rubpy-ph₃-Si(CH₃)₃](PF₆)₂ (**1**)

A solution of [Rubpy-ph-Br] (190.5 mg, 18.8 mmol), 4'-trimethylsilylbiphenyl-4-boronic acid (53.5 mg, 19.8 mmol) and K₂CO₃ in DMF (30 mL) was degassed three times by freeze-pump-thaw technique. Subsequently Pd(PPh₃)₄ (15.4 mg, 0.013 mmol) was added and the reaction mixture was heated at 95 °C. After 16 h the solvent was removed under vacuum and the residue was purified by silica gel chromatography (eluent: MeCN/H₂O/MeOH/NaCl, 4:1:1:0.1). An orange-red powder was obtained after evaporation of the solvents (yield: 93%). ¹H NMR (300 MHz, CD₃CN): δ = 8.77 (s, 1H), 8.69 (d, ³J = 8.3 Hz, 1H), 8.49 (dd, ³J = 13 Hz, ³J = 7.8 Hz, 4H), 8.04 (m, 5H), 7.94 (dd, ³J = 19.5 Hz, ³J = 8.5 Hz, 4H), 7.88–7.56 (m, 15H), 7.39 (m, ³J = 6.0 Hz, 5H), 0.33 (s, 9H). ESI-MS, *m/z*: 1015.21 (*M*⁺ − PF₆), 435.12 (*M*⁺ − 2PF₆).

5.4.2. [Rubpy-ph₃-I](PF₆)₂ (**2b**)

At 0 °C, ICl (35 mg, 0.22 mmol) in CH₂Cl₂ (2 mL) was added to a solution of [Rubpy-ph₃-Si(CH₃)₃](PF₆)₂ (101 mg, 0.087 mmol) in CH₂Cl₂ (20 mL). After 1.5 h the ice-bath was removed and the reaction mixture was stirred for another 1.5 h at room temperature. A solution of Na₂S₂O₃ (1 M in H₂O, 10 mL) and NH₄PF₆ (0.5 g in 5 mL H₂O) was added and the reaction mixture was stirred for 20 min. The two phases are separated and the organic layer was washed with water (2 × 20 mL), brine (10 mL) and dried over MgSO₄. Evaporation of the solvent yielded an orange powder (yield: 98%). ¹H NMR (300 MHz, CD₃CN): δ = 8.86 (s, 1H), 8.79 (d, ³J = 8.0 Hz, 1H), 8.59 (m, 4H), 8.16–7.92 (m, 9H), 7.91–7.72 (m, 13H), 7.54 (d, ³J = 8.3 Hz, 2H), 7.50–7.41 (m, 5H). ESI-MS, *m/z*: 1069.07 (*M*⁺ − PF₆), 462.05 (*M*⁺ − 2PF₆).

5.4.3. [Rubpy-ph₄-I](PF₆)₂ (**2c**)

At 0 °C, ICl (27 mg, 0.16 mmol) in CH₂Cl₂ (2 mL) was added to a solution of [Rubpy-ph₄-Si(CH₃)₃](PF₆)₂ (85 mg,

0.066 mmol) in CH_2Cl_2 (20 mL). Followed by a similar workup procedure as for [Rubpy- $\text{ph}_3\text{-I}$](PF_6)₂ (yield: 99%). ¹H NMR (300 MHz, CD_3CN): δ = 8.82 (s, 1H), 8.73 (d, ³*J* = 6.5 Hz, 1H), 8.54 (dd, ³*J* = 6.8 Hz, ³*J* = 5.7 Hz, 4H), 8.16–8.06 (m, 5H), 8.05–7.96 (m, 4H), 7.92–7.72 (m, 17H), 7.53 (d, ³*J* = 8.4 Hz, 2H), 7.49–7.40 (m, 5H). ESI-MS, *m/z*: 1145.11 ($M^+ - \text{PF}_6$), 500.07 ($M^+ - 2\text{PF}_6$).

5.4.4. [Rubpy- $\text{ph}_3\text{-bpy}$](PF_6)₂ (**3b**)

[Rubpy- $\text{ph}_2\text{-I}$] (115 mg, 0.097 mmol), 4[4(4,4,5,5-tetramethyl-[1,3,2]dioxaborolan-2-yl)-[2,2']bpyridinyl] (38 mg, 0.011 mmol) and K_2CO_3 (80 mg, 0.58 mmol) were dissolved in DMF (20 mL) and the system was degassed three times by freeze-pump-thaw technique. Finally $\text{Pd}(\text{PPh}_3)_4$ (11 mg, 0.010 mmol) were added and the solution was heated at 95 °C for 6 h. The DMF was evaporated and the compound was washed with water (2 × 20 mL) and diethylether (2 × 20 mL) prior to column chromatography on silica gel with $\text{MeCN}/\text{H}_2\text{O}/\text{MeOH}/\text{NaCl}$, 4:1:1:0.1 as eluent (yield: 65%). ¹H NMR (300 MHz, CD_3CN): δ = 8.85–8.69 (m, 5H), 8.61–8.51 (m, 5H), 8.18–7.58 (m, 26H), 7.51–7.41 (m, 6H). ESI-MS, *m/z*: 1097.20 ($M^+ - \text{PF}_6$), 476.13 ($M^+ - 2\text{PF}_6$).

5.4.5. [Rubpy- $\text{ph}_4\text{-bpy}$](PF_6)₂ (**3c**)

[Rubpy- $\text{ph}_3\text{-I}$] (100 mg, 0.082 mmol), 4[4(4,4,5,5-tetramethyl-[1,3,2]dioxaborolan-2-yl)-[2,2']bpyridinyl] (44 mg, 0.124 mmol) and K_2CO_3 (68 mg, 0.49 mmol) were dissolved in DMF (15 mL) and the system was degassed three times by freeze-pump-thaw technique. Finally $\text{Pd}(\text{PPh}_3)_4$ (10 mg, 0.008 mmol) were added and the solution was heated at 95 °C for 6 h. The DMF was evaporated and the compound was washed with water (2 × 20 mL) and diethylether (2 × 20 mL) prior to column chromatography on silica gel with $\text{MeCN}/\text{H}_2\text{O}/\text{MeOH}/\text{NaCl}$, 4:1:1:0.1 as eluent (yield: 75%). ¹H NMR (300 MHz, CD_3CN): δ = 8.86–8.69 (m, 5H), 8.61–8.50 (m, 5H), 8.18–7.70 (m, 29H), 7.66–7.58 (m, 1H), 7.52–7.41 (m, 6H). ESI-MS, *m/z*: 1173.27 ($M^+ - \text{PF}_6$), 514.15 ($M^+ - 2\text{PF}_6$).

5.4.6. [Rubpy- $\text{ph}_5\text{-bpy}$](PF_6)₂ (**3d**)

[Rubpy- $\text{ph}_4\text{-I}$] (62 mg, 0.048 mmol), 4[4(4,4,5,5-tetramethyl-[1,3,2]dioxaborolan-2-yl)-[2,2']bpyridinyl] (23 mg, 0.063 mmol) and K_2CO_3 (40 mg, 0.29 mmol) were dissolved in DMF (15 mL) and the system was degassed three times by freeze-pump-thaw technique. Finally $\text{Pd}(\text{PPh}_3)_4$ (5.5 mg, 0.005 mmol) were added and the solution was heated at 95 °C for 6 h. The DMF was evaporated and the compound was washed with water (2 × 20 mL) and diethylether (2 × 20 mL) prior to column chromatography on silica gel with $\text{MeCN}/\text{H}_2\text{O}/\text{MeOH}/\text{NaCl}$, 4:1:1:0.1 as eluent (yield: 78%). ¹H NMR (300 MHz, CD_3CN): δ = 8.85–8.69 (m, 5H), 8.61–8.49 (m, 5H), 8.18–7.70 (m, 34H), 7.54–7.41 (m, 6H). ESI-MS, *m/z*: 1249.31 ($M^+ - \text{PF}_6$), 552.16 ($M^+ - 2\text{PF}_6$).

5.5. General procedure for the synthesis of heterodinuclear Ru/Os complexes

5.5.1. [Ru- $\text{ph}_2\text{-Os}$](PF_6)₄ (**4a**)

[Rubpy- $\text{ph}_2\text{-bpy}$](PF_6)₂ (42 mg, 0.036 mmol) was added to $\text{Os}(\text{bpy})_2\text{Cl}_2$ (30 mg, 0.049 mmol) dissolved in ethylene glycol (5 mL). The suspension was repeatedly heated three times for 2 min in a standard microwave oven (450 W), allowing cooling down between heating periods. The solvent was removed under reduced pressure to a solid residue. The crude product was dissolved in water/acetone (1:1, 10 mL), and a saturated aqueous solution of NH_4PF_6 was added. The acetone was removed under reduced pressure from the water phase and the precipitated solid was filtered, washed with water (3 × 20 mL) and diethylether (2 × 20 mL). The crude product was dissolved in acetone (3 mL), and purified over silica gel chromatography with $\text{MeCN}/\text{H}_2\text{O}/\text{MeOH}/\text{NaCl}$, 4:1:1:0.1, as eluent to yield a dark-green powder (yield: 82%). ¹H NMR (400 MHz, CD_3CN): δ = 8.82 (dd, ³*J* = 8.08 Hz, ⁴*J* = 1.5 Hz, 2H), 8.73 (dd, ³*J* = 8.08 Hz, 2H), 8.54 (ddd, ³*J* = 8.08 Hz, 8H), 8.15–8.07 (m, 5H), 8.04 (dd, ³*J* = 8.08 Hz, ⁴*J* = 3.03 Hz, 4H), 7.99 (d, ³*J* = 8.08 Hz, 4H), 7.95–7.86 (m, 4H), 7.85 (d, ³*J* = 6.06 Hz, 1H), 7.83–7.67 (m, 15H), 7.65 (dd, ³*J* = 6.06 Hz, ⁴*J* = 1.5 Hz, 1H), 7.48–7.42 (m, 5H), 7.39–7.33 (m, 5H). ESI-MS, *m/z*: 834.16 ($M^+ - 2\text{PF}_6$), 508.45 ($M^+ - 3\text{PF}_6$), 344.59 ($M^+ - 4\text{PF}_6$).

5.5.2. [Ru- $\text{ph}_3\text{-Os}$](PF_6)₄ (**4b**)

[Rubpy- $\text{ph}_3\text{-bpy}$](PF_6)₂ (29 mg, 0.023 mmol) was added to $\text{Os}(\text{bpy})_2\text{Cl}_2$ (21 mg, 0.035 mmol) dissolved in ethylene glycol (5 mL) and irradiated three times 2 min in a microwave oven (450 W) (yield: 87%). ¹H NMR (300 MHz, CD_3CN): δ = 8.82 (dd, ³*J* = 6.9 Hz, 2H), 8.73 (t, ³*J* = 7.35 Hz, 2H), 8.53 (m, 8H), 8.16–7.87 (m, 21H), 7.86–7.62 (m, 15H), 7.45 (m, 5H), 7.33 (m, 5H). ESI-MS, *m/z*: 873.14 ($M^+ - 2\text{PF}_6$), 533.10 ($M^+ - 3\text{PF}_6$), 364.09 ($M^+ - 4\text{PF}_6$).

5.5.3. [Ru- $\text{ph}_4\text{-Os}$](PF_6)₄ (**4c**)

[Rubpy- $\text{ph}_4\text{-bpy}$](PF_6)₂ (50 mg, 0.038 mmol) was added to $\text{Os}(\text{bpy})_2\text{Cl}_2$ (34 mg, 0.057 mmol) dissolved in ethylene glycol (5 mL) and irradiated three times 2 min in a microwave oven (450 W) (yield: 85%). ¹H NMR (400 MHz, CD_3CN): δ = 8.83 (dd, ³*J* = 8.08 Hz, ⁴*J* = 1.5, 2H), 8.74 (dd, ³*J* = 8.08 Hz, 2H), 8.54 (ddd, ³*J* = 8.08 Hz, 8H), 8.16–8.07 (m, 5H), 8.04 (dd, ³*J* = 8.08 Hz, ⁴*J* = 3.53 Hz, 4H), 7.99 (d, ³*J* = 8.08 Hz, 4H), 7.91 (s, 12H), 7.86 (d, ³*J* = 6.06 Hz, 1H), 7.84–7.67 (m, 13H), 7.66 (dd, ³*J* = 6.06 Hz, ⁴*J* = 1.5 Hz, 1H), 7.48–7.42 (m, 5H), 7.40–7.33 (m, 5H). ESI-MS, *m/z*: 911.17 ($M^+ - 2\text{PF}_6$), 558.46 ($M^+ - 3\text{PF}_6$), 382.85 ($M^+ - 4\text{PF}_6$).

5.5.4. [Ru- $\text{ph}_5\text{-Os}$](PF_6)₄ (**4d**)

[Rubpy- $\text{ph}_5\text{-bpy}$](PF_6)₂ (20 mg, 0.014 mmol) was added to $\text{Os}(\text{bpy})_2\text{Cl}_2$ (10 mg, 0.016 mmol) dissolved in ethylene glycol (5 mL) and irradiated three times 2 min in a microwave oven (450 W) (yield: 80%). ¹H NMR (300 MHz, CD_3CN): δ = 8.83 (dd, ³*J* = 9.20 Hz, ⁴*J* = 1.6, 2H), 8.74 (t, ³*J* = 8.40 Hz,

2H), 8.54 (q, $^3J = 7.60$ Hz, 8H), 8.16–8.07 (m, 5H), 8.04 (dd, $^3J = 8.08$ Hz, $^4J = 3.53$ Hz, 4H), 7.99 (d, $^3J = 8.08$ Hz, 4H), 7.91 (m, 16H), 7.85 (d, $^3J = 6.06$ Hz, 1H), 7.84–7.67 (m, 13H), 7.66 (m, 1H), 7.46–7.45 (m, 5H), 7.38–7.33 (m, 5H). ESI-MS, m/z : 949.74 ($M^+ - 2PF_6$), 583.52 ($M^+ - 3PF_6$), 402.03 ($M^+ - 4PF_6$).

5.6. Alternative synthetic route for

5.6.1. [Ru-ph₂-Os](PF₆)₄ (**4a**)

Ru(bpy)₂Cl₂ (120 mg, 0.24 mmol) and 4[4(4,4,5,5-tetramethyl-[1,3,2]dioxaborolan-2-yl)-[2,2']bipyridinyl] (80 mg, 0.22 mmol) were dissolved in dry methoxy ethanol (5 mL). The solution was heated at 90 °C for 18 h under Argon. The reaction mixture was cooled to room temperature and the solvent was removed under reduced pressure. The crude product was washed with hexane (4 × 20 mL) in order to remove the organic starting material. The flask was then loaded with [Os(bpy-ph-Br)(PF₆)₂] (246 mg, 0.22 mmol), K₂CO₃ (500 mg, 3.61 mmol) and degassed DMF (15 mL). Finally the catalyst Pd(PPh₃)₄ (0.04 mol%) was added. The reaction mixture was heated at 100 °C for 22 h. The solvent was evaporated under reduced pressure to afford a black green solid. The crude product was purified by column chromatography (SiO₂) with MeCN/H₂O/MeOH/KNO₃, 4:1:1:0.1 as eluent, preparative plate (SiO₂, MeCN/H₂O/MeOH/KNO₃, 4:1:1:0.1, as mobile phase) and recrystallisation from acetone/diethylether. (**4a**) was obtained as a crystalline dark-green powder (yield: 42%).

Acknowledgments

This research was supported by Philips Research (Contract No. RWC-061-JR-00084-jr) and the European Union (MWFM G5RD-CT-2002-00776).

References

- [1] F. Scandola, C. Chiorboli, M.T. Indelli, M.A. Rampi, in: V. Balzani (Ed.), *Electron Transfer in Chemistry: Covalently Linked Systems Containing Metal Complexes*, vol. III, Wiley, Weinheim, 2001, p. 337.
- [2] J.P. Launay, C. Coudret, in: V. Balzani (Ed.), *Electron Transfer in Chemistry: Wires Based on Metal Complexes*, vol. V, Wiley, Weinheim, 2001, p. 3.
- [3] M.D. Ward, C.M. White, F. Barigelletti, N. Armaroli, G. Calogero, L. Flamigni, *Coord. Chem. Rev.* 171 (1998) 481.
- [4] M.D. Ward, F. Barigelletti, *Coord. Chem. Rev.* 216 (2001) 127.
- [5] L. De Cola, P. Belser, in: V. Balzani (Ed.), *Electron Transfer in Chemistry: Photonic Wires Containing Metal Complexes*, vol. 5, Wiley/VCH Verlag GmbH, Weinheim/Germany, 2001, p. 97.
- [6] L. De Cola, P. Belser, *Coord. Chem. Rev.* 177 (1998) 301.
- [7] F. Barigelletti, L. Flamigni, V. Balzani, J.-P. Collin, J.-P. Sauvage, A. Sour, E.C. Constable, A. Thompson, *Coord. Chem. Rev.* 132 (1994) 209.
- [8] B. Schlicke, L. De Cola, P. Belser, V. Balzani, *Coord. Chem. Rev.* 208 (2000) 267.
- [9] L. Flamigni, F. Barigelletti, N. Armaroli, J.-P. Collin, I.M. Dixon, J.-P. Sauvage, J.A.G. Williams, *Coord. Chem. Rev.* 192 (1999) 671.
- [10] M.T. Indelli, F. Scandola, J.-P. Collin, J.-P. Sauvage, A. Sour, *Inorg. Chem.* 35 (1996) 303.
- [11] M. Staffilani, P. Belser, F. Hartl, C.J. Kleverlaan, L. De Cola, *J. Phys. Chem. A* 106 (2002) 9242.
- [12] B. Schlicke, P. Belser, L. De Cola, E. Sabbioni, V. Balzani, *J. Am. Chem. Soc.* 121 (1999) 4207.
- [13] L. De Cola, V. Balzani, F. Barigelletti, L. Flamigni, P. Belser, S. Bernhard, *Recl. Trav. Chim. Pays-Bas-J. R. Neth. Chem. Soc.* 114 (1995) 534.
- [14] J.-P. Sauvage, J.-P. Collin, J.-C. Chambron, S. Guillerez, C. Coudret, V. Balzani, F. Barigelletti, L. De Cola, L. Flamigni, *Chem. Rev.* 94 (1994) 993.
- [15] L. De Cola, V. Balzani, F. Barigelletti, L. Flamigni, P. Belser, A. Von Zelewsky, M. Frank, F. Vögtle, *Mol. Cryst. Liq. Cryst. Sci. Technol. Sect. A: Mol. Cryst. Liq. Cryst.* 252 (1994) 97.
- [16] L. De Cola, V. Balzani, F. Barigelletti, L. Flamigni, P. Belser, A. Von Zelewsky, M. Frank, F. Vögtle, *Inorg. Chem.* 32 (1993) 5228.
- [17] L. De Cola, F. Barigelletti, V. Balzani, R. Hage, J.G. Haasnoot, J. Reedijk, J.G. Vos, *Chem. Phys. Lett.* 178 (1991) 491.
- [18] A. Harriman, M. Hissler, A. Khatyr, R. Ziessel, *Eur. J. Inorg. Chem.* (2003) 955.
- [19] A. El-ghayoury, A. Harriman, R. Ziessel, *J. Phys. Chem. A* 104 (2000) 7906.
- [20] A. Juris, L. Prodi, A. Harriman, R. Ziessel, M. Hissler, A. El-ghayoury, F.Y. Wu, E.C. Riesgo, R.P. Thummel, *Inorg. Chem.* 39 (2000) 3590.
- [21] V. Grossshenny, A. Harriman, F.M. Romero, R. Ziessel, *J. Phys. Chem.* 100 (1996) 17472.
- [22] V. Grossshenny, A. Harriman, R. Ziessel, *Angew. Chem. Int. Ed. Engl.* 34 (1995) 1100.
- [23] M. Tsushima, N. Ikeda, K. Nozaki, T. Ohno, *J. Phys. Chem. B* 104 (2000) 5176.
- [24] J.-P. Collin, P. Gavina, V. Heitz, J.-P. Sauvage, *Eur. J. Inorg. Chem.* (1998) 1.
- [25] F. Barigelletti, L. Flamigni, M. Guardigli, A. Juris, M. Beley, S. Chodorowski-Kimmes, J.-P. Collin, J.-P. Sauvage, *Inorg. Chem.* 35 (1996) 136.
- [26] F. Barigelletti, L. Flamigni, V. Balzani, J.-P. Collin, J.-P. Sauvage, A. Sour, *New J. Chem.* 19 (1995) 793.
- [27] R.L. Paul, A.F. Morales, G. Accorsi, T.A. Miller, M.D. Ward, F. Barigelletti, *Inorg. Chem. Commun.* 6 (2003) 439.
- [28] E.C. Constable, R.W. Handel, C.E. Housecroft, A.F. Morales, L. Flamigni, F. Barigelletti, *Dalton Trans.* (2003) 1220.
- [29] S. Encinas, L. Flamigni, F. Barigelletti, E.C. Constable, C.E. Housecroft, E.R. Schofield, E. Figgemeier, D. Fenske, M. Neuburger, J.G. Vos, M. Zehnder, *Chem. Eur. J.* 8 (2002) 137.
- [30] M. Furue, T. Yoshidzumi, S. Kinoshita, T. Kushida, S. Nozakura, M. Kamachi, *Bull. Chem. Soc. Jpn.* 64 (1991) 1632.
- [31] M. Furue, K. Maruyama, Y. Kanematsu, T. Kushida, M. Kamachi, *Coord. Chem. Rev.* 132 (1994) 201.
- [32] M.D. Hossain, M. Haga, B. Gholamkhash, K. Nozaki, M. Tsushima, N. Ikeda, T. Ohno, *Collect. Czech. Chem. Commun.* 66 (2001) 307.
- [33] F. Barigelletti, L. Flamigni, V. Balzani, J.-P. Collin, J.-P. Sauvage, A. Sour, E.C. Constable, A. Thompson, *J. Am. Chem. Soc.* 116 (1994) 7692.
- [34] L. Hammarstrom, F. Barigelletti, L. Flamigni, M.T. Indelli, N. Armaroli, G. Calogero, M. Guardigli, A. Sour, J.-P. Collin, J.-P. Sauvage, *J. Phys. Chem. A* 101 (1997) 9061.
- [35] M.T. Indelli, F. Scandola, L. Flamigni, J.-P. Collin, J.-P. Sauvage, A. Sour, *Inorg. Chem.* 36 (1997) 4247.
- [36] C. Patoux, J.-P. Launay, M. Beley, S. Chodorowski-Kimmes, J.-P. Collin, S. James, J.-P. Sauvage, *J. Am. Chem. Soc.* 120 (1998) 3717.
- [37] Y.Y. Liang, A.I. Baba, W.Y. Kim, J. Atherton, R.H. Schmehl, *J. Phys. Chem.* 100 (1996) 18408.

- [38] W.B. Davis, W.A. Svec, M.A. Ratner, M.R. Wasielewski, *Nature* 396 (1998) 60.
- [39] K. Kalyanasundaram, *Photochemistry of Polypyridine and Porphyrine Complexes*, Academic Press, London, 1994.
- [40] T. Akasaka, H. Inoue, M. Kuwabara, T. Mutai, J. Otsuki, K. Araki, *Dalton Trans.* (2003) 815.
- [41] J. Andersson, F. Puntoriero, S. Serroni, A. Yartsev, T. Pascher, T. Polivka, S. Campagna, V. Sundstrom, *Chem. Phys. Lett.* 386 (2004) 336.
- [42] F. Barigelletti, L. Flamigni, *Chem. Soc. Rev.* 29 (2000) 1.
- [43] A. Beyeler, P. Belser, *Coord. Chem. Rev.* 230 (2002) 29.
- [44] A.K. Bilakhiya, B. Tyagi, P. Paul, *Polyhedron* 19 (2000) 1233.
- [45] C. Chiorboli, M.A.J. Rodgers, F. Scandola, *J. Am. Chem. Soc.* 125 (2003) 483.
- [46] E.C. Constable, E. Figgemeier, C.E. Housecroft, J. Olsson, Y.C. Zimmermann, *Dalton Trans.* (2004) 1918.
- [47] P.T. Gulyas, T.A. Smith, M.N. Paddon-Row, *J. Chem. Soc., Dalton Trans.* (1999) 1325.
- [48] R.T.F. Jukes, V. Adamo, F. Hartl, P. Belser, L. De Cola, *Inorg. Chem.* 43 (2004) 2779.
- [49] L.S. Kelso, T.A. Smith, A.C. Schultz, P.C. Junk, R.N. Warrener, K.P. Ghiggino, F.R. Keene, *J. Chem. Soc., Dalton Trans.* (2000) 2599.
- [50] S.J.A. Pope, C.R. Rice, M.D. Ward, A.F. Morales, G. Accorsi, N. Armaroli, F. Barigelletti, *J. Chem. Soc., Dalton Trans.* (2001) 2228.
- [51] F. Puntoriero, S. Serroni, A. Licciardello, M. Venturi, A. Juris, V. Ricevuto, S. Campagna, *J. Chem. Soc., Dalton Trans.* (2001) 1035.
- [52] S. Rau, B. Schafer, S. Schebesta, A. Grussing, W. Poppitz, D. Walther, M. Duati, W.R. Browne, J.G. Vos, *Eur. J. Inorg. Chem.* (2003) 1503.
- [53] F. Weldon, L. Hammarstrom, E. Mukhtar, R. Hage, E. Gunneweg, J.G. Haasnoot, J. Reedijk, W.R. Browne, A.L. Guckian, J.G. Vos, *Inorg. Chem.* 43 (2004) 4471.
- [54] T. Tzalis, *J. Am. Chem. Soc.* 119 (1997) 852.
- [55] E. Baranoff, I.M. Dixon, J.-P. Collin, J.-P. Sauvage, B. Ventura, L. Flamigni, *Inorg. Chem.* 43 (2004) 3057.
- [56] M. Fukuda, K. Sawada, K. Yoshino, *J. Polym. Sci., Polym. Chem.* 31 (1993) 2465.
- [57] S. Welter, A. Benetti, N. Rot, N. Salluze, P. Belser, P. Sonar, A.C. Grimsdale, K. Müllen, M. Lutz, A.L. Spek, L. De Cola, submitted for publication.
- [58] E.M. Kober, J.V. Caspar, R.S. Lumpkin, T.J. Meyer, *J. Phys. Chem.* 90 (1986) 3722.
- [59] I.B. Berlmann, *Handbook of Fluorescence Spectra of Aromatic Compounds*, Academic Press, London, 1965.
- [60] S.L. Murov, P. Carmichael, G.L. Hug, *Handbook of Photochemistry*, Dekker, New York, 1993.
- [61] D.L. Dexter, *Chem. Phys.* 21 (1953) 836.
- [62] A. Helms, D. Heiler, G. McLendon, *J. Am. Chem. Soc.* 114 (1992) 6227.
- [63] E.A. Weiss, M.J. Ahrens, L.E. Sinks, A.V. Gusev, M.A. Ratner, M.R. Wasielewski, *J. Am. Chem. Soc.* 126 (2004) 5577.
- [64] R.E. Holmlin, R.F. Ismagilov, R. Haag, V. Mujica, A.M. Ratner, M.A. Rampi, G.M. Whitesides, *Angew. Chem. Int. Ed.* 40 (2001) 2316.
- [65] E.M. Kober, J.V. Caspar, B.P. Sullivan, T.J. Meyer, *Inorg. Chem.* 27 (1988) 4587.
- [66] V. Hensel, A.D. Schlüter, *Liebigs Ann./Receuil* (1997) 303.
- [67] O. Bossart, L. De Cola, S. Welter, G. Calzaferri, *Chem. Eur. J.* 10 (2004) 5771.